Journal of the Franklin Institute 361 (2024) 106971

Contents lists available at ScienceDirect

Journal of the Franklin Institute

journal homepage: www.elsevier.com/locate/fi

Auto-tuning method for PI controllers under Symmetric-Send-on-Delta sampling strategy

Julio-Ariel Romero-Pérez, Oscar Miguel-Escrig *

Department of System Engineering and Design, Universitat Jaume I, Campus del Riu Sec, Avda. Vicent Sos Baynat s/n 12071, Castelló de la Plana, Spain

ARTICLE INFO

Keywords:
Auto-tuning
Event-based-PID
SSOD
Robustness

ABSTRACT

In this work, an auto-tuning method for PI controllers applied in a loop under a Symmetric-Send-On-Delta sampling strategy is proposed. Auto-tuning algorithms usually implement an identification phase to obtain some information about the system dynamic that is used for tuning the controller. In our proposal, two frequency response points are estimated through an iterative procedure. With this information, a simple tuning rule is applied which guarantees robustness against limit cycle oscillations that can be induced by the SSOD sampler. Both the robustness measure to limit cycles and the identification procedure are based on the describing function technique, whose validity in the networked control systems under study requires a low incidence of losing packets as well as the transmission delays to be known or negligible compared to the system's dynamic. Comparatives with other classical tuning rules support the suitability of the proposed method. The auto-tuning procedure has been validated through a simulation study reflecting its applicability for the most common dynamics found in industrial processes.

1. Introduction

In recent years, Event-Based Control (EBC) in its different variants is becoming an alternative to classical control schemes [1], offering execution patterns other than the periodic call to the control algorithms. This change in the execution aims to reduce the measurement frequency, saving resources usage, such as communication, actuators, average computation cost and, ultimately, energy, without degrading the closed-loop performance. Fields of application of EBC principles are networked control systems or cyber physical systems, where many devices share a communication network. For example in [2], EBC has been applied and has proved its effectiveness while reducing the power consumption of remote sensors.

The effectiveness of EBC, in terms of performance and expected behavior, is determined, together with the control algorithms, by the event generation technique. This fact is shown in [3] where a comparative study of control loops considering different event generation techniques is presented. These event generation techniques are in charge of monitoring the state of the system and, when a significant change is produced, sending an event to trigger the execution of the control algorithms. Techniques based on level-crossing are a common choice for its ease of implementation. Send-On-Delta (SOD) strategy, introduced in [4], was one of the firsts contributions in this aspect. This technique consists on sending events when a change greater than the threshold δ is observed from the last value sent, and it has been tested in terms of loop performance and communication reduction [5,6].

In [7], a variation in SOD sampling was presented, called Symmetric-Send-On-Delta (SSOD). The main characteristic of this sampling strategy is that the quantization levels are fixed, being multiples of the threshold δ, including a hysteresis of the same

* Corresponding author.
E-mail addresses: romeroj@uji.es (J.-A. Romero-Pérez), omiguel@uji.es (O. Miguel-Escrig).

https://doi.org/10.1016/j.jfranklin.2024.106971
Received 6 September 2022; Received in revised form 30 December 2023; Accepted 2 June 2024
Available online 22 June 2024

magnitude δ. The effectiveness of the SSOD sampling in networked control systems has been evaluated through its use in several actual applications in processes control [8,9], as well as in laboratory scale systems [10–13], where, among other applications, mechatronic systems exhibiting rapid variations were studied, demonstrating the validity of the SSOD sampling even in those cases. Beyond its applications in distributed control loops, the use of this kind of sampling in non-distributed control systems could be boosted in the next few years by the recent development of level-crossing analog to digital converters, motivated by the increasing necessity of low-power consumer electronic devices in the context of the IoT [14]. In this sense, some works have addressed the electronic implementation of level-crossing converters with hysteresis [15,16], which are a particular case of the SSOD sampling.

Limit cycle oscillations are an undesired behavior that can be induced by the SSOD sampling technique, therefore, in several works tuning rules have been proposed assuring robustness against their induction [11,17–20]. Most of these works use the Describing Function (DF) technique [21] as a base for the studies, but there exist other analysis tools available, like Tsypkin's method [22], which has also been used to provide a tuning rule not only for PI but also for PID controllers, [18]. Other works use the SSOD induced oscillations for identification purposes [23–25]. However, to the knowledge of authors, the problem of auto-tune algorithms in the context of SSOD based control systems has not been successfully addressed in previous works.

Auto-tuning algorithms consist of two phases, firstly, an identification phase is developed to obtain some information about the dynamic of the system, then, a tuning rule is applied which takes into account the information obtained in the identification phase. Once the controller is tuned, the control loop is closed for controlling the system. Hitherto, the studies about auto-tuning methods for SSOD based PI controllers has been scarce, being the contribution in [24] the most remarkable in the field. In that work, a procedure was presented to identify the process transfer function whose structure must be previously selected. The identification procedure is based on the oscillatory response induced by the SSOD sampler. Once the transfer function is obtained, it is used to calculate the PI parameters. The oscillations to identify the transfer function take place after introducing a PI controller tuned by the Ziegler–Nichols method from a relay feedback experiment developed in the beginning of the procedure.

In this work, an auto-tuning method is proposed for PI controllers applied in SSOD sampled control loops. The procedure does not require the estimation of parametric models, such as the process transfer function, which has always been needed in the previous tuning methods reported in the literature. Instead, it is only required to identify two points of the system's frequency response to perform the tuning. Those points are obtained from oscillations induced by a relay with hysteresis plus an integrator introduced in the loop containing the SSOD sampler. With this information, the controller's parameters are obtained according to an ad-hoc proposed tuning rule which provides an user-defined robustness degree against limit cycle oscillations through a single parameter. This tuning rule has been compared with other classical well-known tuning rules, namely, Ziegler–Nichols [26], AMIGO [27], One-Third [28] and SIMC [29] tuning rules; in terms of robustness and performance. The comparison proves the suitability of the proposed method to deal with very different kind of dynamic behaviors, which describe most of the actual industrial systems. The resulting tuning rules are intended to be easy to implement and, therefore, to apply in any industrial device

The paper is organized as follows. In Section 2, the loop configuration considered in this paper with its characteristics is presented. The proposed tuning rule is detailed in Section 3, where a comparison with other classical tuning rules is included supporting the tuning rule validity. Section 4 describes the identification phase of the auto-tuning method. Here two options for obtaining the information needed for the tuning rule are studied: firstly, using the oscillation induced by the SSOD, and secondly, using the oscillation induced by a relay plus time delay. The results show that the later option presents significant advantages over the former one in terms of experiment duration and predictable behavior. A simulation study to validate the proposal is presented in Section 5. Finally, the conclusions about the work are drawn in Section 6.

2. Loop characteristics

The loop configuration considered in this paper is presented in Fig. 1. It consists of a sensor unit with an Event Generator (EG) that transmits the data through the network whose behavior is modeled with a time delay term, and the controller and actuator unit which holds the received data with a Zero-Order Hold (ZOH), and computes the control action with the algorithms implemented in the controller $C(s)$ whose output is applied to the process to control with unknown transfer function $G_p(s)$. To facilitate the study, the elements in the loop are re-arranged by combining the EG and ZOH in a single block and considering the network delay as part of the unknown transfer function giving by Eq. (1).

$$G(s) = G_p(s)\exp(-t_d s) \tag{1}$$

In this work, the event generation is in charge of a Symmetric-Send-On-Delta (SSOD) sampler [7], which constitutes a specific case of the Send-On-Delta. The behavior of this event generator, according to its input–output relationship, is described by:

$$\bar{e}(t) = \begin{cases} (i+1)\delta & \text{if} \quad e(t) \geq (i+1)\delta \quad \text{and} \quad \bar{e}(t^-) = i\delta, \quad i \in \mathbb{Z} \\ (i-1)\delta & \text{if} \quad e(t) \leq (i-1)\delta \quad \text{and} \quad \bar{e}(t^-) = i\delta \\ i\delta & \text{if} \quad e(t) \in [(i-1)\delta, (i+1)\delta] \quad \text{and} \quad \bar{e}(t^-) = i\delta \end{cases} \tag{2}$$

where $e(t)$ is the error signal (input) that generates the sampled error signal $\bar{e}(t)$ (output) and δ the quantification level.

Regarding to its input–output relationship, the SSOD can be considered as a multilevel relay with hysteresis. The robustness against the induction of limit cycle oscillations induced by this kind of non-linear elements can be characterized by means of the Describing Function technique, as firstly proposed in [30] and after exploited in other works for different studies as commented in the previous section. It is assumed for this work a sampling frequency high enough to correctly capture the system's dynamics.

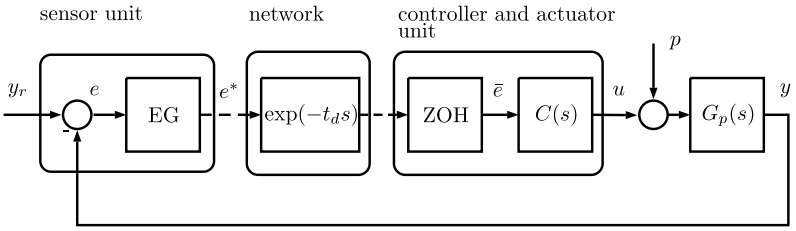

Fig. 1. Standard loop configuration for EBC.

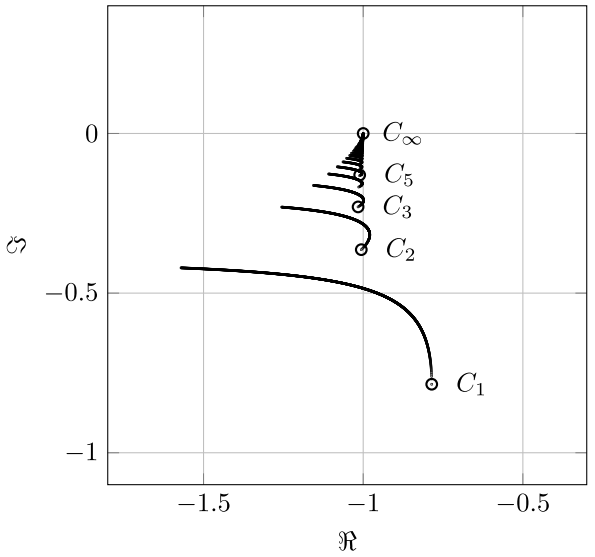

Fig. 2. Representation of $-1/\mathcal{N}(A)$ of the SSOD in the Nyquist plane.

Cases where this assumption is not fulfilled fall outside the scope of this work since the stability of these loops must be studied differently as shown in [31].

The Describing Function (DF) of the SSOD-ZOH sampling and hold strategy, which was firstly obtained in [11], results in the following expression:

$$\mathcal{N}(A) = \frac{2\delta}{A\pi}\left[1 + \sqrt{1-\left(\frac{\delta}{A}m\right)^2} + 2\sum_{k=1}^{m-1}\sqrt{1-\left(\frac{\delta}{A}k\right)^2}\right] - j\frac{2m\delta^2}{A^2\pi}, \tag{3}$$

where A is the amplitude of a sinusoidal input to the SSOD, and $m = \lfloor A/\delta \rfloor$ is the maximum number of levels crossed in either direction. DF theory states that limit cycles can be induced in the temporal response if the open-loop transfer function intersects the inverse negative of the DF at any frequency, which can be expressed analytically as:

$$G_{ol}(j\omega) = -\frac{1}{\mathcal{N}(A)}, \quad \forall\omega$$

where $G_{ol}(j\omega) = C(j\omega)G(j\omega)$ is the open-loop transfer function.

The traces of the inverse negative of the DF are presented in Fig. 2 for $A \in [\delta, \infty[$. In that figure, some points C_i are highlighted, which represent the points where $A = i\delta$, e.g. the point C_1 is obtained calculating $-1/\mathcal{N}(\delta)$ and C_2 from $-1/\mathcal{N}(2\delta)$. Each of these points are then followed by a trace which are the result of computing the inverse negative of the DF for $A \in [i\delta, (i+1)\delta[$. An intersection of the open-loop transfer function with each of these traces can induce a limit cycle oscillation in the temporal response with the corresponding amplitude A at the open-loop transfer function frequency at which the intersection is produced.

Some studies based on the DF method try to avoid limit cycle oscillations by establishing robustness margins to the point $C_1 = -\pi/4 - j\pi/4$, which is the point of minimum amplitude of oscillation $A = \delta$. As has been proved in [11], by avoiding the intersection with the trace corresponding to the point C_1 also prevent the intersection with the rest of traces of the negative inverse of the DF, so oscillation will not take place. Therefore, the point C_1 can be considered as critical point for properly tuning the controller.

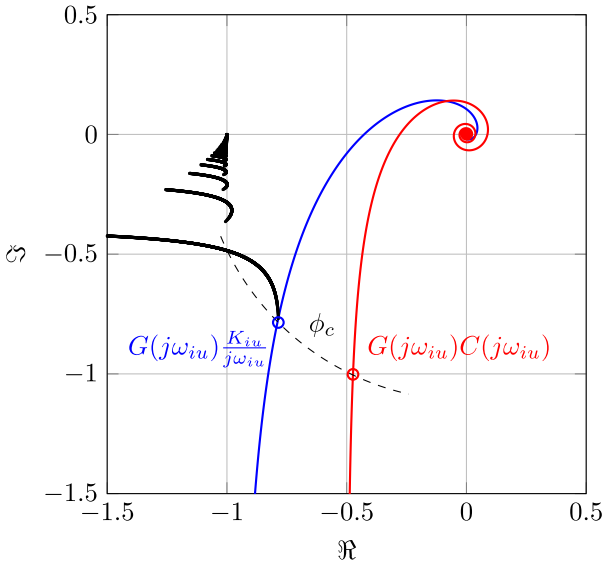

Fig. 3. Tuning method rationale establishing a phase margin ϕ_c to the point C with a PI controller. (For interpretation of the references to color in this figure legend, the reader is referred to the web version of this article.)

3. Tuning method

The key point for any auto-tuning procedure is to dispose of a method for calculating the controller parameters using information easily obtained from a suitable test over the system, like a relay feedback experiment. With this in mind, a very simple tuning method is proposed in this section that only requires some information related to the critical point C_1.

Let us assume the open loop transfer function $\hat{G}_{ol}(j\omega) = G(j\omega)\frac{K_{iu}}{j\omega}$ resulting from replacing the controller $C(s)$ by an integrator with a properly selected gain K_{iu} such that $\hat{G}_{ol}$ crosses the point C_1 in some frequency ω_{iu}, which is the frequency of oscillation induced by the SSOD if $\hat{G}_{ol}$ intercepts $-1/\mathcal{N}(A)$ in C_1.

$$G(j\omega_{iu})\frac{K_{iu}}{j\omega_{iu}} = G(j\omega_{iu})I(j\omega_{iu}) = C_1 = -\frac{\pi}{4} - j\frac{\pi}{4} \tag{4}$$

The rationale of the tuning method consists on substituting the integrator with gain, $I(j\omega)$, by a PI controller in the open-loop transfer function, obtaining the controllers' parameters that assure a custom phase margin ϕ_c to the point C_1 at the frequency ω_{iu} as it is shown in Fig. 3, where $\hat{G}_{ol}(j\omega) = G(j\omega)I(j\omega)$ is presented in blue and $G_{ol}(j\omega) = G(j\omega)C(j\omega)$ in red.

The design parameter ϕ_c allows establishing a robustness margin against the induction of limit cycle oscillations while adding some extra margin against potential errors on the estimation of the critical point C_1, which can be derived from actual plant problems like network latency or packet losses.

Remark 1. It is worth noticing that the phase margin to the oscillations ϕ_c is measured respect to point $C_1 = 1.11\angle{-135°}$ and it must be distinguished from the classical phase margin specification Φ, measured respect to $1\angle{180°}$. Because $|C_1| = 1.11$ is close to 1, the following relation is fulfilled: $\phi_c \approx \Phi - 45°$. Therefore, when designing with $\phi_c \in [5°, 25°]$ will approximately produce values of the classical phase margin $\Phi \in [50°, 70°]$, which are reasonable values for this robustness measurement. The previous relation between Φ and ϕ_c has been studied and validated in [30,32].

For a PI controller with transfer function

$$C(j\omega) = K_p + \frac{K_i}{j\omega}, \tag{5}$$

the parameters K_p and K_i that assure the described behavior are obtained as follows:

$$\begin{aligned} K_p &= \frac{K_{iu}}{\omega_{iu}}\sin\phi_c \\ K_i &= K_{iu}\cos\phi_c \end{aligned} \tag{6}$$

being K_p and K_i the proportional and integral gain of the controller and where ϕ_c is the phase margin to the point C_1. The calculation behind this tuning rule is detailed in Appendix A.

The main advantage of the tuning rules in Eq. (6) in order to be used in an auto-tuning procedure is that it does not require the identification of the plant model $G(s)$, instead, the controller parameters' can be calculated from data that can be extracted

from simple relay feedback experiments, as will be presented in the next section. In addition, it provides a customizable degree of robustness against limit cycles provided by the phase margin to the point C_1 characterized by ϕ_c, allowing the user to obtain more robust controllers if required.

In order to compare the proposed tuning method with other well known tuning rules, a study has been made focusing on classical specifications such as gain margin γ, phase margin Φ or settling time T_s and the phase margin to the point C_1, ϕ_c. A batch of processes involving the most common dynamics, presented in Eqs. (7), has been considered to perform the comparison. Note that according to Eq. (1) $G(s)$ include both the process transfer function and the network delay, therefore this batch includes cases in which the network delays are taken into account and others cases where the delay introduced by the network can be neglected respect to the process dynamic.

$$
\begin{aligned}
&G(s) = \frac{e^{-s}}{(Ts+1)^2},\\
&T = 0.01, 0.02, 0.05, 0.1, 0.2, 0.3, 0.5, 0.7, 1,\\
&\quad 1.3, 1.5, 2, 4, 6, 8, 10, 20, 50, 100, 200, 500\\
&G(s) = \frac{1}{(s+1)(Ts+1)^2},\\
&T = 0.05, 0.1, 0.2, 0.5, 2, 5, 10\\
&G(s) = \frac{1}{(s+1)^n},\\
&n = 3, 4, 5, 6, 7, 8\\
&G(s) = \frac{1}{(s+1)(\alpha s+1)(\alpha^2 s+1)(\alpha^3 s+1)},\\
&\alpha = 0.1, 0.2, 0.3, 0.4, 0.5, 0.6, 0.7, 0.8, 0.9\\
&G(s) = \frac{Te^{-L_1 s}}{(T_1 s+1)(Ts+1)}, \quad T_1 + L_1 = 1,\\
&T = 1, 2, 5, 10 \quad L_1 = 0.01, 0.02, 0.05, 0.1, 0.3, 0.5, 0.7, 0.9, 1\\
&G(s) = \frac{1-\alpha s}{(s+1)^3},\\
&\alpha = 0.1, 0.2, 0.3, 0.4, 0.5, 0.6, 0.7, 0.8, 0.9, 1, 1.1\\
&G(s) = \frac{1}{(s+1)((sT)^2 + 1.4sT + 1)},\\
&T = 0.1, 0.2, 0.3, 0.4, 0.5, 0.6, 0.7, 0.8, 0.9, 1
\end{aligned}
\tag{7}
$$

With the models proposed in the batch, several controllers have been tuned according to the following methods: Ziegler–Nichols [26], AMIGO [27], One-Third [28] and SIMC [29], and also by the proposed method assuming $\phi_c = 20°$. By choosing this value for ϕ_c it is foreseen to obtain values of the classical phase margin Φ close to 65°, as commented in Remark 1.

The results are presented in Fig. 4. As expected, the proposed method presents values of Φ around 65°, similar to those values obtained for the SIMC method. With regard to the gain margin, the proposal provides values in the order of magnitude of the other methods.

Concerning the settling time T_s, the collected data has been normalized with regard to SIMC's settling time, which presents, in average, the fastest responses. The proposed method presents settling times in the same range as the classical methods, even presenting in some cases the fastest responses. As expected, the phase margin to the point C_1 is set to 20° degrees for the proposed method, being variable for the classical tuning methods, specially for Ziegler–Nichols'.

Summarizing, the proposed method is suitable for tuning the controller $C(s)$ for most of the processes in industry under the control scheme in Fig. 1, providing characteristics similar to the ones provided by classical methods while it guarantees robustness to limit cycles induced by the SSOD sampler. To be applied, the presented tuning method only needs the information of the integral gain K_{iu} and the oscillation frequency ω_{iu} which can be obtained from the limit cycle oscillations induced by the non-linearity in the loop, as will be presented in the next section.

4. Identification of the critical oscillation point parameters K_{iu} and ω_{iu}

The aim of the identification procedure proposed in this section is to obtain the gain K_{iu} of the integrator and the frequency ω_{iu} at which the open-loop transfer function, defined by the process and the integrator, intersects the point C_1, that is, the values of K_i and ω fulfilling the condition in Eq. (8), which is graphically represented in Fig. 5.

$$
G(j\omega_{iu})\frac{K_{iu}}{j\omega_{iu}} = C_1 \tag{8}
$$

Because the point C_1 belong to $-\frac{1}{\mathcal{N}(A)}$, one could use the oscillations induced by the SSOD non linearity in the closed loop systems presented in Fig. 1, after substituting the controller $C(s)$ by an integrator $I(s)$, in order to obtain K_{iu} and ω_{iu}. However, trying to perform this identification with the SSOD sampler requires to apply a trial and error procedure for selecting values of K_i

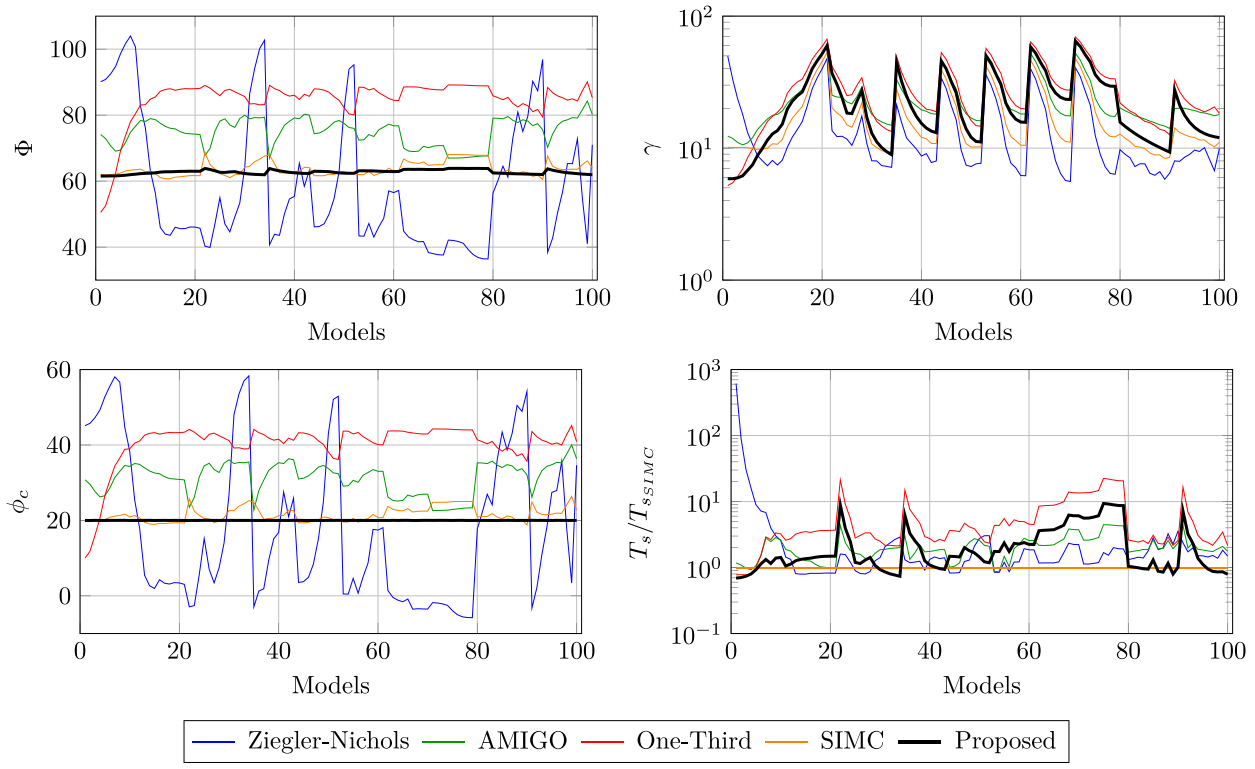

Fig. 4. Comparative of the robustness and performance of the proposed tuning method with classical tuning rules. (For interpretation of the references to color in this figure legend, the reader is referred to the web version of this article.)

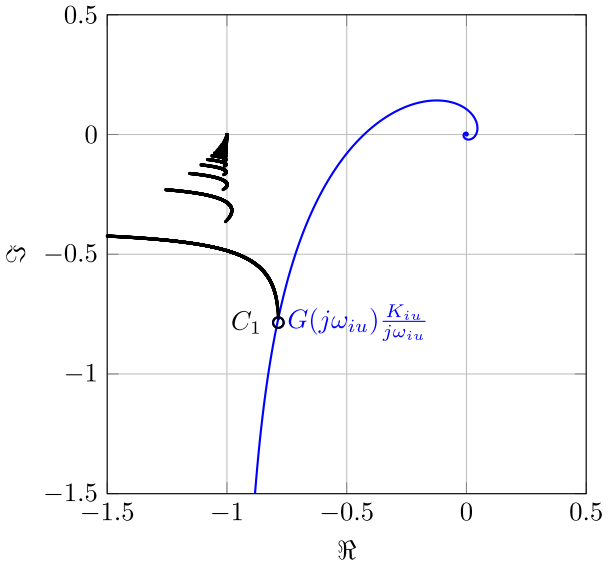

Fig. 5. Intersection of the open-loop transfer function $G(j\omega)I(j\omega)$ with the point C_1.

until the limit cycle corresponding to C_1 is reached. From the practical point of view this approach presents several drawbacks. Firstly, there exists the possibility of obtaining an unstable behavior, which can happen if for the selected value of K_i the open-loop transfer function intersects the Nyquist's abscissa axis in a value lower than -1. Secondly, a stable state can be reached, in which no oscillation is obtained, if the selected value of K_i does not guarantee intersection between the open-loop transfer function and the inverse negative of the DF. Additionally, during the blind search of K_{iu}, if $G(j\omega)K_i/j\omega$ intercepts several traces of $-\frac{1}{\mathcal{N}(A)}$, then the oscillatory response of the system can take place in any of the limits cycles corresponding to the intersections points, each one

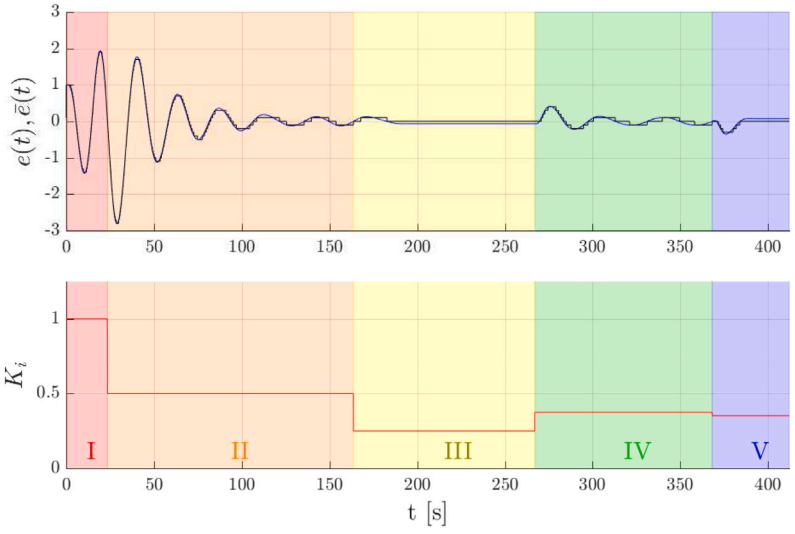

Fig. 6. Experimental deployment of the auto-tuning procedure based on the SSOD binary search.

with its own properties of amplitude and frequency. This huge variability in the system responses when using the SSOD sampler to look for the oscillation in point C_1 could cause long and unfeasible experiments, making this approach theoretically viable, but hardly applied in actual systems. The following example illustrates this fact.

Example 1. Fig. 6 shows an experiment that presents some situations described above. The approach to obtain the oscillation point C_1 in this experiment consists in a binary search of K_{iu}. The values of K_i through the experiment until K_{iu} is obtained in phase IV are shown in the figure. In the initial phase I, an arbitrary integral gain is set, and the process becomes unstable. Therefore, the integral gain is reduced in phase II, where a stable oscillation is obtained, but since its amplitude is higher than δ, which is the amplitude of oscillation in the point C_1 needed to estimate K_{iu} and ω_{iu}, the experiment continues reducing the integral gain in phase III. In this phase, the process reaches a stable state, thus, in phase IV the integral gain is increased to produce new oscillations. These last oscillations with amplitude close to δ are suitable to obtain K_{iu} and ω_{iu}. Then the controller parameters are calculated by Eqs. (6). Finally, a disturbance is introduced in phase V to test the controller.

The Nyquist diagram in Fig. 7 shows the open loop transfer function in each phase of the experiment. Initially, $G(j\omega)I(j\omega)$, encircle the point (−1,0), therefore oscillations with increasing amplitude are obtained in phase I, as depicted in Fig. 6. The reduction of K_i in phase II produce a new intersection point between $G(j\omega)I(j\omega)$ and $-\frac{1}{\mathcal{N}(A)}$ far from C_1. A further reduction of the integrator gain in phase III avoid this intersection, and consequently the limit cycle oscillation disappears. Then, K_i is increased, resulting in a limit cycle close to C_1 where K_{iu} and ω_{iu} are finally obtained.

In order to overcome the aforementioned issues when using the SSOD sampler to obtain the parameters K_{iu} and ω_{iu}, we propose to estimate the point C_1' of $G(j\omega)I(j\omega)$ with the same phase that point C_1, that is $-3\pi/4$ [rad], see Fig. 8. Once this point is known, K_{iu} can be calculated by Eq. (9). Furthermore, because $C_1 = K_{iu}C_1'$, the oscillation frequency for the point C_1' is equal to ω_{iu}.

$$K_{iu} = \frac{|C_1|}{|C_1'|} = \frac{\pi\sqrt{2}/4}{|C_1'|} \tag{9}$$

The procedure for identifying point C_1' is inspired by the algorithm described in [33] where a single relay is combined with a variable time delay to estimate a point in the frequency response with a given phase. At the beginning of the experiment the delay is set to zero and the point C_0 in Fig. 8 is estimated from the resulting oscillations. The estimation of C_0 is used to calculate the time delay needed to identify the point C_1'. The loop composition to develop the identification is depicted in Fig. 9. As can be seen, a relay with hysteresis is inserted in the loop after the SSOD, followed by a time delay and an integrator. These three elements are implemented in the auto-tuning algorithm in the controller device. Since $G(s) = G_p(s)\exp(-t_d s)$, the effect of communication delay t_d introduced by the network is taking into account as part the system response to be identified.

Due to the input/output characteristic of the relay with hysteresis, which is shown in Fig. 10, if the hysteresis is $h = n_\delta\delta$, $n_\delta \in \mathbb{Z}$, then the non-linearity resulting from the SSOD and relay combination is equivalent to a relay with hysteresis. This means that the introduction of the relay with $h = n_\delta\delta$ in the loop cancels the effect of the SSOD sampler, and consequently, the induced oscillations are fully defined by the relay parameters. This allows developing the identification phase of the auto-tuning procedure without modifying neither removing the SSOD sampler.

Remark 2. Although the condition $h = n_\delta\delta$ is theoretically feasible, its practical implementation could lead to some numerical problems since h is used in the switching condition of the relay to check if the input signal, which is a quantized signal with levels

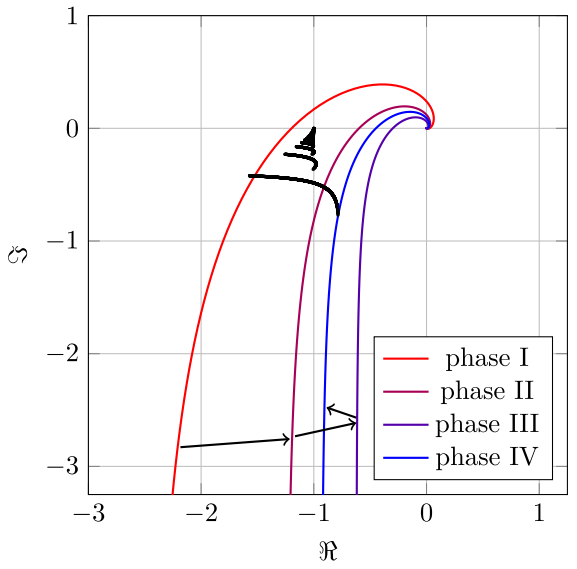

Fig. 7. Binary search of the intersection between the open-loop transfer function and the point C_1.

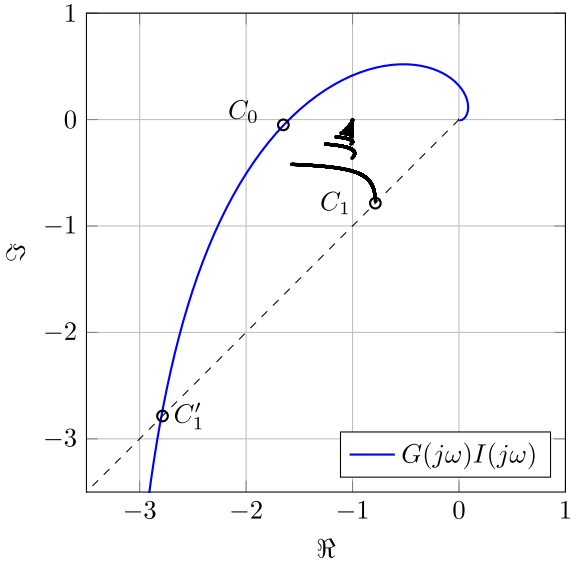

Fig. 8. Relay-based search of the characteristics of the intersection between $G_{ol}(s)$ and C_1.

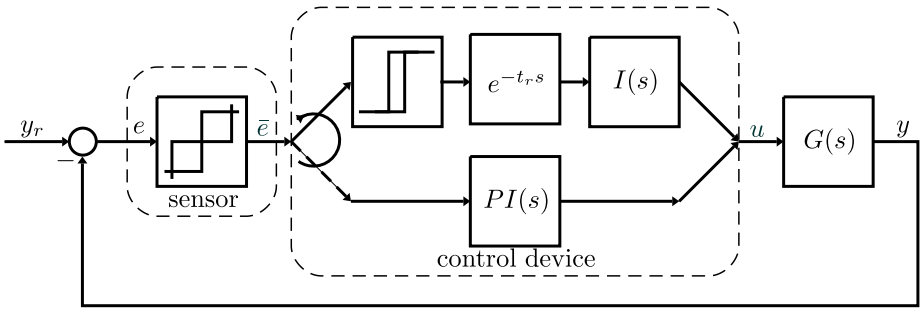

Fig. 9. Loop modification for the identification and control phases when using the relay plus delay approach for identifying the point C_1'.

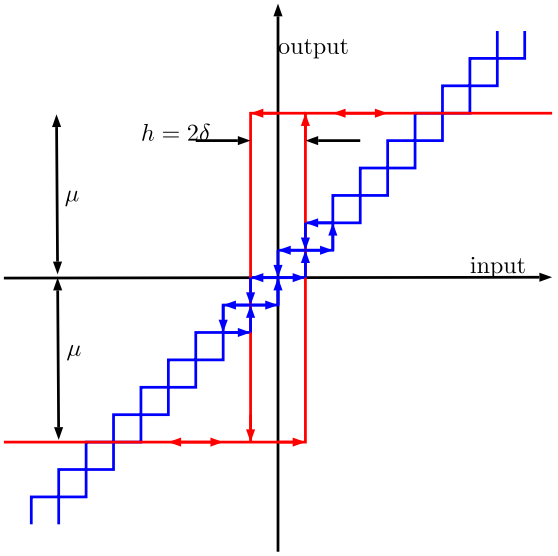

Fig. 10. Input/output characteristic of relay (red) and SSOD (blue). (For interpretation of the references to color in this figure legend, the reader is referred to the web version of this article.)

$n\delta$, $n \in \mathbb{Z}$, has crossed the value $n_\delta\delta$ in order to change the output signal. It is worth noting, however, that since the relay input is a quantized signal, it is expected that the relay output changes after a step-like variation in $\bar{e}$ from $(n_\delta - 1)\delta$ to $n_\delta\delta$. Therefore, h could have any value in the interval $](n_\delta - 1)\delta,\ n_\delta\delta[$. A reasonable value for h is the midpoint of the previous interval: $h = n_\delta\delta - \delta/2$. This guarantees the cancellation of the SSOD effect in the loop meanwhile avoiding the numerical fragility due to the condition $h = n_\delta\delta$.

As commented before, the relay, the time delay and an integrator are implemented in the controller device where the auto-tune algorithm is executed. It is worth noting from Fig. 9, that the controller input is not the error e but the sampled error $\bar{e}$. However, the equations for estimating frequency response points from relay experiments depend on the amplitude A of the oscillation of e, see for example [34]. Instead, the available information for the auto-tuning algorithm is the amplitude $\bar{A}$ of the sampled error $\bar{e}$. This could introduce errors in the estimation of point C_1', which must be reduced as much as possible.

Despite the value of A, the absolute error in its measurement from $\bar{e}$ is in the range $[0, \delta]$. Consequently, the relative error between A and $\bar{A}$,

$$e_A = \frac{A - \bar{A}}{A} 100\% \tag{10}$$

can be reduced by increasing de oscillation amplitude A. Assuming that $\bar{A} = n_A\delta$, being $n_A = \left\lfloor \frac{A_0}{\delta} \right\rfloor \in \mathbb{Z}$ the number of levels δ included in the oscillation amplitude, the upper bound of e_A is $e_A = 1/(1 + n_A)100\%$ (see proof in Appendix B). For $n_A = 1$ the relative error e_A could be up to 50%, however, as n_A rises, e_A can be approximated by $e_A \approx 1/n_a 100\%$. As an example, for $n_A = 10$ the upper bound of the relative error is approximately 10%.

The previous discussion about the error between A and $\bar{A}$ must be taken into account in the proposed algorithm. In this sense, our proposal is based on calculating the relay amplitude μ in order to obtain the oscillation that fulfills the condition $n_A \geq n_{A_d}$, where n_{A_d} is the desired value of n_A. It is worth noting that, in general, an excessive oscillation amplitude is not desired in actual plants, hence, the selection of μ must be a trade off between a low value of e_A and a reasonable oscillation amplitude in the plant output. As commented before, $n_A = 10$ implies $e_A \approx 10\%$, so n_A greater than 10 could be a reasonable choice. Because at the beginning of the experiment there is no information about the process dynamic, the initial value of the relay amplitude, μ_0, should be selected low enough to guarantee admissible oscillation from the process operation point of view. If under this premise the obtained $\bar{A}_0 = n_{A_0}\delta$ does not fulfill the condition $n_{A_0} \geq n_{A_d}$, then the relay amplitude is recalculated by Eq. (11) (see Appendix B for proof) and a new relay experiment is carried out. Eq. (11) can be applied successively until the condition $n_A \geq n_{A_d}$ is fulfilled, then the point C_0 can be estimated.

$$\mu = \mu_0 \frac{n_{A_d}}{n_{A_0} + 1} \tag{11}$$

Remark 3. For most of the actual systems the magnitude of $G(j\omega)I(j\omega)$ decreases when the frequency increases, hence, the magnitude of C_1' is greater than the magnitude of C_0. Then, taking into account that the amplitude of the oscillation is proportional to the magnitude of open loop transfer function, the condition $n_A > n_{A_d}$ is expected to be fulfilled during the experiments for the identification of C_1'. Therefore, the relay amplitude does not change during these experiments, keeping the value obtained for the identification of C_0.

The auto-tuning procedure that takes into account all the previous issues is as follows:

1. Initially the delay is set to zero: $t_r = 0$. A relay feedback experiment with relay hysteresis $h = \delta$ and amplitude low enough to keep the oscillation of the system output in a safety region is carried out resulting in oscillations of frequency ω and amplitude $\bar{A}$. Calculate $n_A = \bar{A}/\delta$, and check the condition $n_A \geq n_{A_d}$. If it is not fulfilled, calculate a new relay amplitude by Eq. (11) and perform a new experiment.
2. Repeat step 1 until the condition $n_A \geq n_{A_d}$ is accomplished. Then, the first identified point (C_0 in Fig. 8) is defined by frequency ω, magnitude $M = \dfrac{\pi\bar{A}}{4\mu}$, and phase $\phi_0 = -\pi - \arg\left(\dfrac{4\mu}{\pi\bar{A}}\left(\sqrt{1-\left(\dfrac{h}{\bar{A}}\right)^2} - j\dfrac{h}{\bar{A}}\right)\right)$. The previous equations are obtained using the describing function of the relay with hysteresis and have been previously used in [34].
3. Set the delay to $t_r = \dfrac{(\phi_d - \phi_0)}{\omega}$, where ϕ_0 has been estimated in the previous step and ϕ_d is the phase of point C_1, that is $-3\pi/4$. Run a new relay feedback experiment, which leads to a new oscillatory response of frequency ω, and amplitude $\bar{A}$. The identified point using these data is defined by frequency ω, magnitude $M = \dfrac{\pi\bar{A}}{4\mu}$ and phase $\phi_G(\omega) = t_r\omega - \pi - \arg\left(\dfrac{4\mu}{\pi\bar{A}}\left(\sqrt{1-\left(\dfrac{h}{\bar{A}}\right)^2} - j\dfrac{h}{\bar{A}}\right)\right)$.
4. Repeat step 3 updating the delay t_r with the new values of ω and ϕ obtained in each iteration until $|\phi_G(\omega) - (-3\pi/4)| < \epsilon$, where ϵ is an admissible error in the phase estimation of point C_1'. The last value of ω and M obtained in step 3 correspond to the point C_1', therefore, $\omega_{iu} = \omega$ and K_{iu} can be calculated according to Eq. (9). A detailed explanation of steps 3 and 4 as well as a convergence study is presented in Appendix C.
5. Finally, the PI parameters are calculated using Eqs. (6) for a given robustness margin ϕ_c.

To measure ω and $\bar{A}$ in each experiment the system output must reach stable oscillations, that is, an oscillation with constant amplitude. Due to the quantization effect of the SSOD sampler, this condition can be easily checked by the equation $\bar{A}_{-1} - \bar{A} = 0$, being $\bar{A}_{-1}$ the penultimate measure of $\bar{A}$.

Remark 4. As a result of the step 1 and Remark 3, the amplitudes of the oscillation obtained in steps 2 and 3 are greater than $n_{A_d}h$, with value of $n_{A_d} > 10$. For $n_{A_d} = 10$ the contribution of the term

$$\arg\left(\frac{4\mu}{\pi\bar{A}}\left(\sqrt{1-\left(\frac{h}{\bar{A}}\right)^2} - j\frac{h}{\bar{A}}\right)\right)$$

in the equations to calculate the phase is only about 0.2 rad. Therefore, this term can be neglected in order to simplify the algorithm without significantly affecting the final result. Hence, in steps 2 the phase ϕ_0 can be approximated by $\phi_0 = -\pi$ and in step 3 the equations for calculating t_r and $\phi_G(\omega)$ can be reduced to

$$t_r = \frac{(\phi_d + \pi)}{\omega} \tag{12}$$

$$\phi_G(\omega) = t_r\omega - \pi \tag{13}$$

The final implementation of the auto-tuning method is summarized in Algorithm 1.

Remark 5. Because the time delay introduced by the network is considered as part of the unknown system model, its variation during the experiments could introduce errors in the estimation of C_1' whose magnitude depends on the relative value of these variations respect to the rest of model parameters. In this sense, it should be noted that in many industrial control applications the plant dynamic is characterized by time lags and delays large enough to neglect the delay introduced by the network. In these cases, the proposed algorithm can be applied. On the other hand, if t_d is on the same order of magnitude as the plant dynamics, then various scenarios are possible. (1) If the variations in the network delay are not significant respect to t_d, the modeling error due to these variations could be neglected, and consequently the algorithm can be applied. (2) If the variations in the network delay are significant respect to t_d, but these variations do not take place during the experiments, that is, t_d is almost constant during the relay tests, then the algorithm can be applied since the robustness margin ϕ_c prevents the induction of limit cycles due to modeling errors. (3) The worst situation is when the variations in the network delay occur during the experiments and are significant respect to the model parameters. In this case, the values of t_r are strongly influenced by the variations in t_d, and therefore, the convergence of relay experiments cannot be guaranteed.

Example 2. In order to show the benefits of using the relay plus delay approach to identify the point C_1', let us consider the process with transfer function

$$G(s) = \frac{0.55}{(s+1)^5}$$

Algorithm 1 Auto-tuning algorithm summary

$\mu \leftarrow \mu_0$
Perform Relay feedback experiment;
while $n_A < n_{A_d}$ **do**
  Update μ; ▷ Equation (11)
  Perform Relay feedback experiment;
end while
$t_r \leftarrow 0$
$\phi_G \leftarrow -\pi$
$\omega \leftarrow$ oscillation frequency from the last experiment
repeat
  Update t_r; ▷ Equation (12)
  Perform Relay feedback experiment
  $\omega \leftarrow$ oscillation frequency from the last experiment
  $\phi_G \leftarrow$ estimated phase ▷ Equation (13)
until $|\phi_G - \phi_d| < \epsilon$
$\omega_{iu} \leftarrow \omega$
Calculate K_{iu}; ▷ Equation (9)
Calculate K_p and T_i; ▷ Equation (6)

whose identification using the SSOD non-linearity was presented in Example 1. The value of δ for SSOD sampler is 0.1. For the identification, a relay with initial amplitude and hysteresis of 0.1 has been considered.

The behavior of the main signals and parameters during the identification and control phases is presented in Fig. 11. The first experiment phase begins at $t = 0$. The vertical lines in the oscillatory stages indicate the end of experiments to identify the points C_0 and C_1'. By comparing Figs. 11 and 6 it can be seen that the total duration of the experiment is significantly reduced. Furthermore, the usage of relay plus time delay guarantees stable oscillations, whose amplitude can be kept under control, avoiding the unstable oscillation as observed in phase I of Fig. 6. Hence, the system repose during the experiments with relay plus time delay is, in general, more predictable than the behavior obtained when using the SSOD to identify the point C_1'.

As it can be seen, during the first phase of the experiment, which lasts 113 s, the time delay is zero and the relay amplitude is recalculated twice to fulfill the condition $n_A \geq n_{A_d}$ with $n_{A_d} = 20$. The values of n_A at the end of each stable oscillation is presented in the bottom figure. In order to reduce the experiment duration, the first phase of the experiment ends once n_A is close enough to n_{A_d}, in this case when $n_A = 18$, and the point C_0 is calculated using the value of $\bar{A}$. During the second phase of the experiment, the time delay is modified to identify the point C_1'. As expected, according to Remark 3, during this phase n_A is greater than the values obtained in the first phase without varying the relay amplitude. Once the point C_1' is identified at the end of the second phase, at 206 s, the controller parameters are calculated considering a margin $\phi_c = 20°$ and the PI algorithm is activated. In order to evaluate the performance of the controller, a disturbance of magnitude 10 is introduced at $t = 300$ s whose effect in the system output is fully compensated by the controller 30 s later.

As it can be seen, there are not limit cycle oscillation in the control loop once the PI is activated, since the controller obtained by the auto-tuning method avoids the intersection between $G_{ol}(j\omega) = C(j\omega)G(j\omega)$ and $-1/\mathcal{N}(A)$ due to the phase margin ϕ_c. This is shown in Fig. 12, where the polar plot of $G_{ol}(j\omega)$ and the negative inverse of the describing function of SSOD are depicted. The estimation of point C_1' is also presented in the figure. The error in the estimation of C_1' is mainly due to the use of the describing function technique, which neglects the effect of higher order harmonics in the loop response.

Remark 6. The error in the estimation of C_1' observed in Example 2 does not reduce the robustness to limit cycles of the controller, conversely, the robustness is increased because $|\hat{C}_1'| > |C_1'|$, and consequently, the value of K_{iu} obtained from Eq. (9) decreases. Therefore, the controller parameters K_p and K_i from Eq. (6) are also reduced. Hence, the effect of the error in the estimation of C_1' is similar to detune the controller obtained with the actual C_1' point, increasing the robustness at the expenses of a slightly slower closed loop response. This fact has been also detected in processes with very different dynamic behavior, as it will be presented in the next section.

5. Simulation study

In this section some examples illustrate the performance of the auto-tuning algorithm for SSOD-PI controllers based on relay plus delay feedback experiments. In order to validate the proposal, a batch of transfer function models including the most common dynamics encountered in industrial processes, presented in Eqs. (14), has been considered. The auto-tuning algorithm has been applied in all these cases with the following parameters: $n_{A_d} = 20$, $\phi_c = 20°$. A SSOD sampler with $\delta = 0.1$ and a relay with initial amplitude and hysteresis of 0.1 has been assumed.

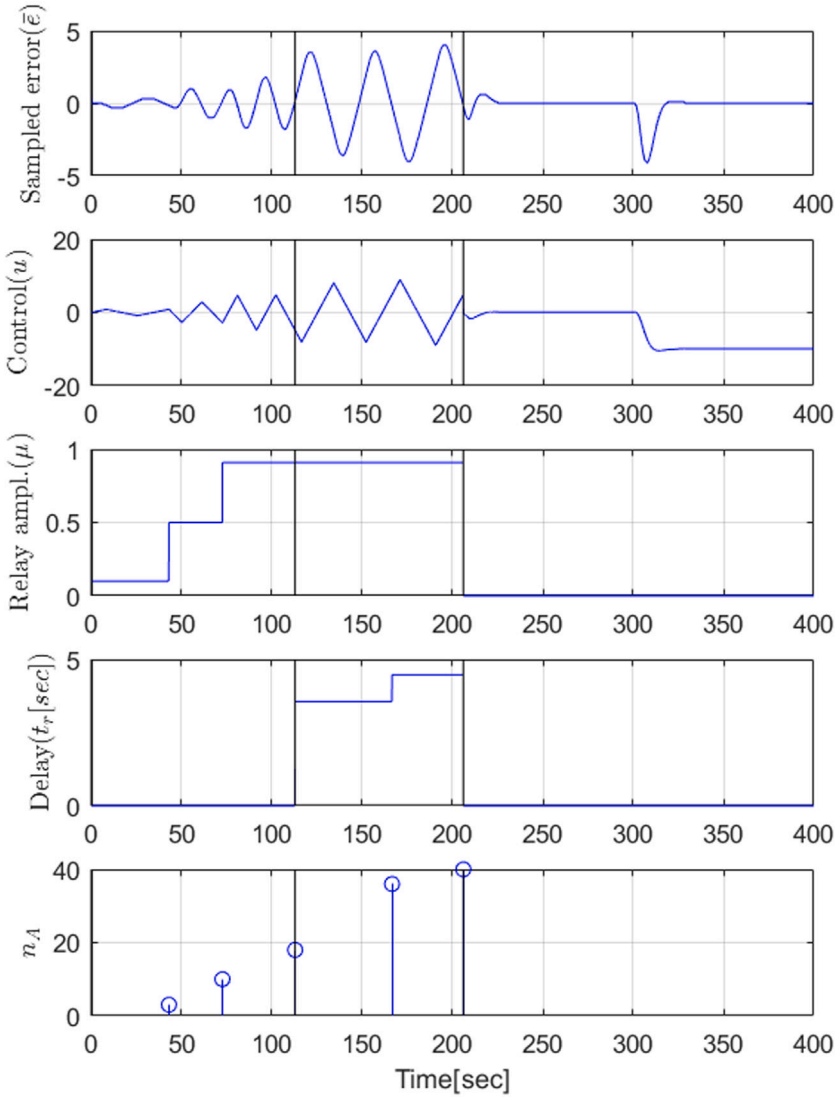

Fig. 11. Time response of the main signals and parameters during the experiment and control phase in Example 2.

$$
\begin{aligned}
G_1(s) &= \frac{e^{-5s}}{(s+1)^3} \\
G_2(s) &= \frac{1}{(s+1)(0.5s+1)(0.25s+1)(0.125s+1)} \\
G_3(s) &= \frac{1}{(s+1)^7} \\
G_4(s) &= \frac{1-2s}{(s+1)^3}
\end{aligned}
\tag{14}
$$

The behavior of the main auto-tuning algorithm parameters is presented in Figs. 13 to 16, where the vertical black lines represent the final of each experimental phase. As it can be seen, during the first phase the time delay t_r is zero and the amplitude of the relay (μ) is adjusted until the condition $n_A = n_{A_d}$ is fulfilled. During the second phase of the experiment the relay amplitude does not change since $n_A > n_{A_d}$ and consequently, the oscillation amplitude can measured from $\bar{e}$ without introducing a significant error. On the other hand, during this phase t_r is recalculated to identify the point C_1'. At the end of this phase the PI parameters K_p and K_i are calculated and the controller algorithm is activated.

The performance of the resulting controllers can be observed in Fig. 16, where the responses to a step disturbance applied at $t = 300$ s is shown. In all cases the effect of this perturbation is rejected and the error between the reference and the measured variable is canceled in a reasonable time. Regarding to the existence of limit cycles, oscillations are not detected in the closed loop responses of the obtained PI. This fact is corroborated by the polar plots in Fig. 17, which depict the frequency response of the

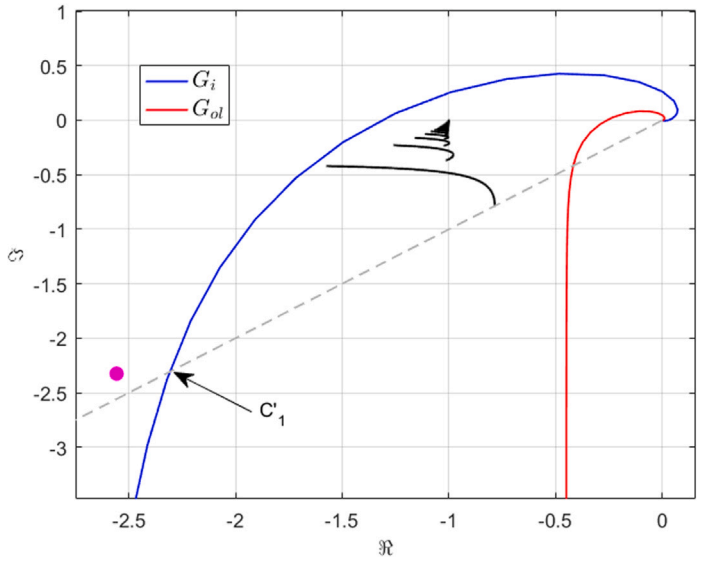

Fig. 12. Polar plot of the transfer functions of Example 2. Magenta circle: estimation of point C_1': $\hat{C}_1'$.

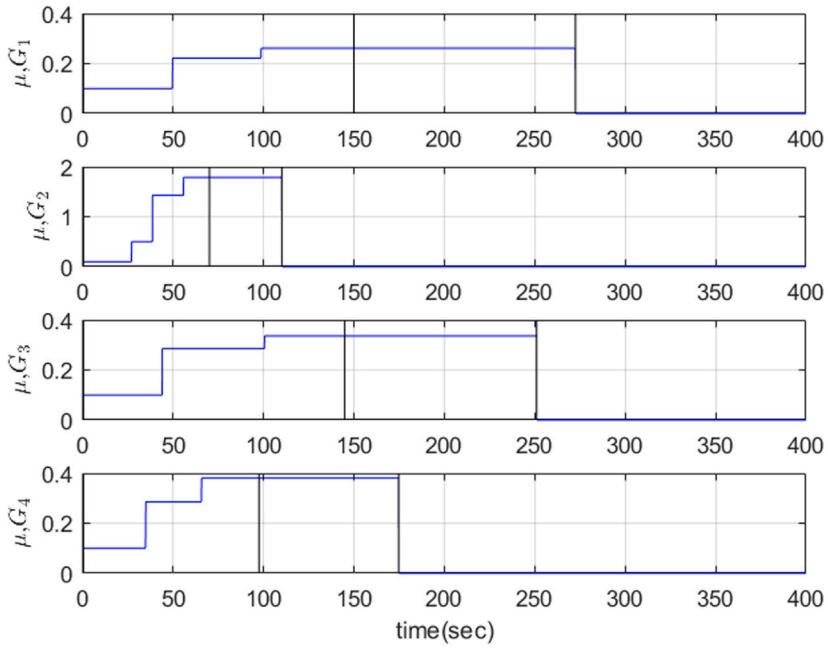

Fig. 13. Relay amplitude (μ) during the auto-tuning procedure for systems with transfer functions in Eq. (14).

open loop transfer function for systems G_1 to G_4. As it can be seen, in all cases G_{ol} does not intercept the negative inverse of the describing function. Furthermore, the tuning parameter ϕ_c guarantees enough robustness margins to avoid such interceptions even if reasonable modeling errors or variation in the systems parameters take place. Finally, from this Figure it is worth noting that in all cases $|\hat{C}_1'| > |C_1'|$. Therefore, the error in the estimation of C_1' does not degrade the robustness to limit cycles, as it has been pointed out in Remark 6.

6. Conclusion

In this paper, an auto-tuning methodology for tuning PI controllers for a SSOD control loop is presented. The identification approach is based on the information extracted from limit cycles induced by a relay. In the first step, the system is placed in a safe

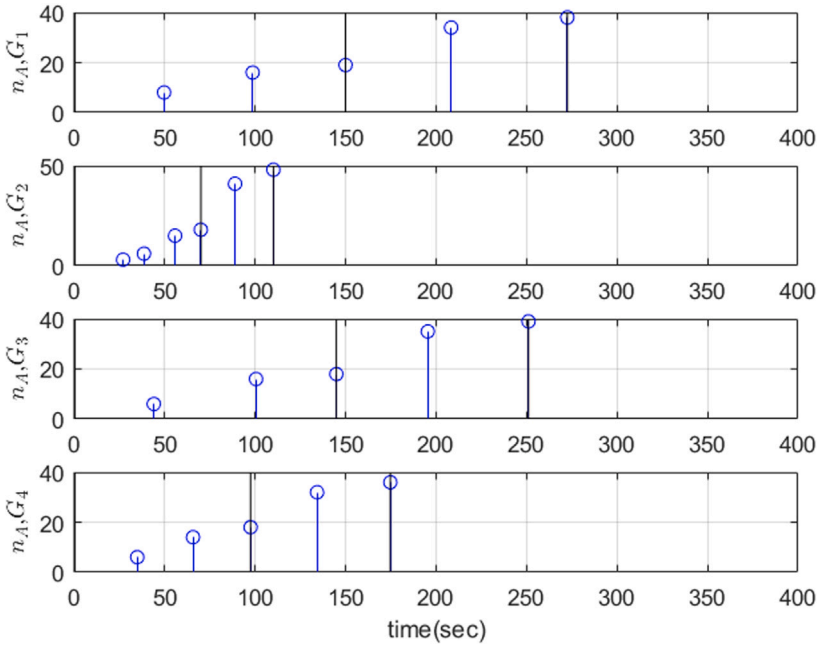

Fig. 14. Oscillation amplitude expressed as number of crossed levels (n_A) during the auto-tuning procedure for systems with transfer functions in Eq. (14).

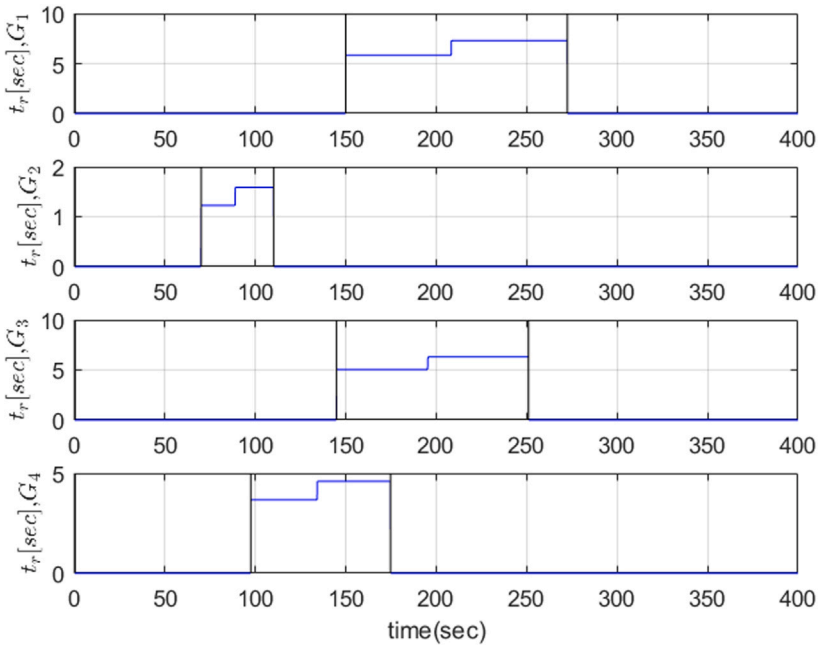

Fig. 15. Time delay (t_r) during the auto-tuning procedure for systems with transfer functions in Eq. (14).

operation region, where the oscillations are controlled. Then, a delay is introduced to obtain the characteristics of a given oscillation, which are used by the tuning method.

With regard to the tuning method, its objective is to establish an user-defined phase margin to the critical point C_1. This is achieved using the information obtained from the identification phase, not needing to obtain a parametric model for tuning the controller. This tuning rule has been compared with other classical tuning rules showing its applicability for SSOD based control loops. Some examples are included showcasing the deployment of the auto-tuning method to processes representing some of the most common dynamics in industry. The simulations show the effectiveness of the proposed procedure.

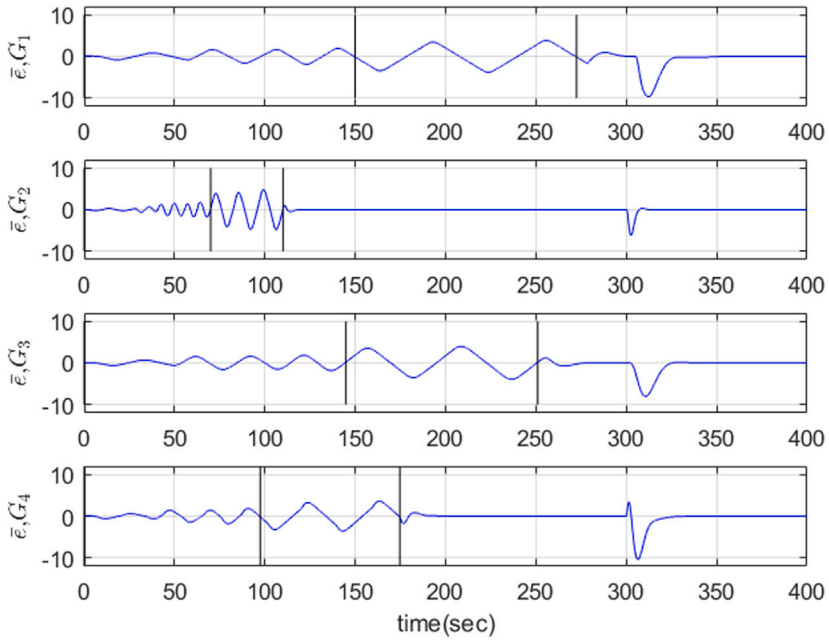

Fig. 16. Sampled error ($\bar{e}$) during the auto-tuning procedure and control phase for systems with transfer functions in Eq. (14).

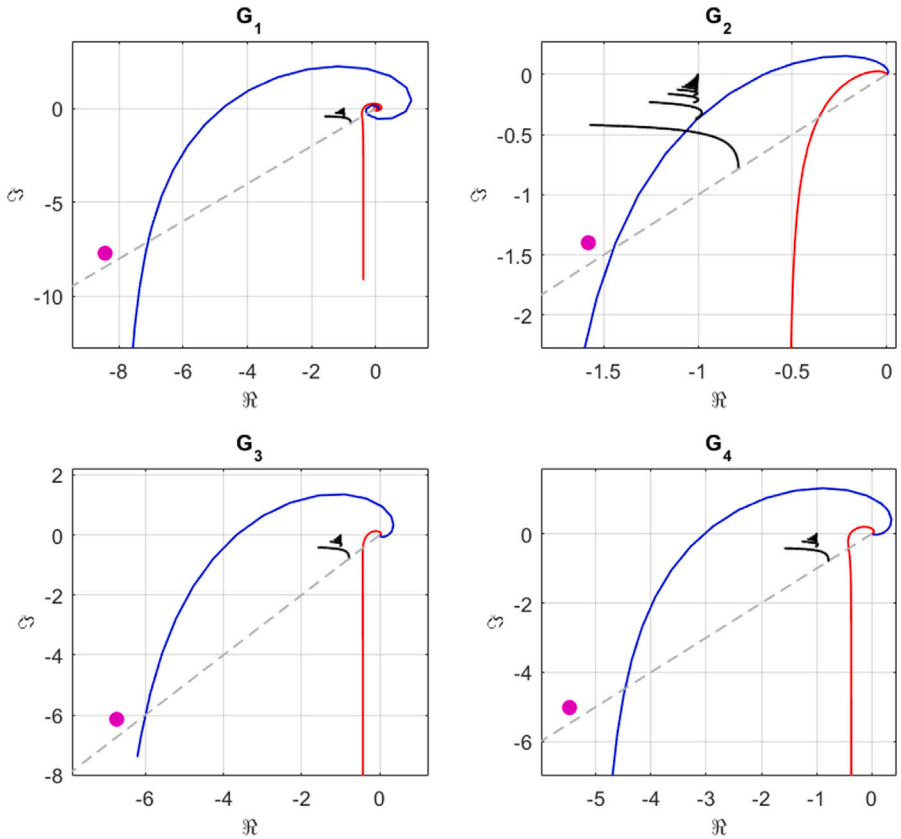

Fig. 17. Polar plot of the transfer functions of systems G_1 to G_4. Blue line: G_i. Red line: G_{ol}. Magenta circles: estimation of point C_1': $\hat{C}_1'$. (For interpretation of the references to color in this figure legend, the reader is referred to the web version of this article.)

It should be remarked that the proposed auto-tune algorithm can be used in general control applications under the following assumptions: (1) The sampling frequency is sufficiently high to capture the system's dynamics (Describing Function theory is applicable) which implies the effects of losing occasional packets being not critical. (2) The plant dynamic is characterized by time lags and delays large enough to neglect the delay introduced by the communication network, or the communication delay must be known if its value is on the same order of magnitude as the plant dynamics. (3) The plant dynamics do not include a pure integrator or unstable poles, those cases fall outside the current study and constitute a possible future work.

This paper has focused on PI controllers, whose use is predominant in many industrial applications due to their simplicity, reliability and ease of tuning. As an example of the prevalence of the PI respect to other kind of controllers, in [35] is reported that more than 95% of control loops in the power industry in China use PI controllers. This widespread application of the PI algorithm reinforce the relevance of the results presented in this paper. Besides, the extension of the proposed algorithm to the PID case must be addressed in future researches, since the inclusion of the derivative term can definitively improve the response in some applications. One of the main issues to obtain a similar auto-tuning method for SSOD based PID is the lack of validity of the describing function approach this case, as has been demonstrated in [18].

Finally, it is worth mentioning that the tuning and auto-tuning of SSOD based discrete controllers, that is controllers with periodic execution, not the continuous case as considered in this paper, is an open issue that must be addressed in future works. In this sense, the existence of limit cycles in this kind of control systems has been studied in [31], however, the design of controllers has not been tackled yet.

Declaration of competing interest

The authors declare that they have no known competing financial interests or personal relationships that could have appeared to influence the work reported in this paper.

Acknowledgments

This work has been supported by research project UJI-B2021-45 from Universitat Jaume I, Spain.

Appendix A. Tuning rule parameters calculation

Consider that the integral gain K_{iu} and the frequency ω_{iu} that fulfill:

$$G(j\omega_{iu})\frac{K_{iu}}{j\omega_{iu}} = -\frac{\pi}{4} - j\frac{\pi}{4} = \frac{\pi}{4}\sqrt{2}\angle -135° \tag{15}$$

are known.

Replacing the integrator by a PI controller and assuming that the same frequency point is to be moved ϕ_c degrees counter-clockwise, that is establishing a phase margin of ϕ_c degrees to the point C_1:

$$G(j\omega_{iu})\left(K_p + \frac{K_i}{j\omega_{iu}}\right) = \frac{\pi}{4}\sqrt{2}\angle -135° + \phi_c \tag{16}$$

Isolating $G(j\omega_{iu})$ from Eq. (15) and replacing it in Eq. (16):

$$\frac{j\omega_{iu}}{K_{iu}}\frac{\pi}{4}\sqrt{2}\angle -135°\left(K_p + \frac{K_i}{j\omega_{iu}}\right) = \frac{\pi}{4}\sqrt{2}\angle -135° + \phi_c$$

equating:

$$K_p j\omega_{iu} + K_i = K_{iu}\angle\phi_c = K_{iu}(\cos\phi_c + j\sin\phi_c)$$

solving K_p and K_i by equalizing to the imaginary and real part respectively:

$$K_p = \frac{K_{iu}}{\omega_{iu}}\sin\phi_c$$
$$K_i = K_{iu}\cos\phi_c$$

Appendix B. Relay amplitude calculation

Assume that the experiment using a relay with amplitude μ_0 produce oscillation of amplitude A_0, whose value after the SSOD sampler is $\bar{A}_0 = n_{A_0}\delta$, $n_{A_0} = \left\lfloor \frac{A_0}{\delta} \right\rfloor$. Then, the oscillation amplitude can be expressed as $A_0 = n_{A_0}\delta + \epsilon_0\delta,\ \epsilon_0 \in]0, 1[$. The relative error between A_0 and $\bar{A}_0$ is:

$$e_{A_0} = \frac{A_0 - \bar{A}_0}{A_0}100\% = \frac{\epsilon_0}{n_{A_0} + \epsilon_0}100\% \tag{17}$$

and for a given value of n_{A_0}, the maximum value of e_{A_0} is obtained for $\epsilon_0 = 1$:

$$e_{A_0} = \frac{1}{n_{A_0} + 1}100\% \tag{18}$$

Taking into account A_0 and μ_0, the magnitude of the negative inverse of the relay describing function can be expressed as,

$$M_0 = \frac{\pi A_0}{4\mu_0} = \frac{\pi(n_{A_0}\delta + \epsilon_0\delta)}{4\mu_0} \tag{19}$$

Furthermore, for any pair (μ, A) of relay amplitude and its corresponding oscillation amplitude, where $A = n_A\delta + \epsilon\delta$, $n_A = \left\lfloor \frac{A}{\delta} \right\rfloor$, $\epsilon \in]0, 1[$, M_0 can be also written as,

$$M_0 = \frac{\pi A}{4\mu} = \frac{\pi(n_A\delta + \epsilon\delta)}{4\mu} \tag{20}$$

Solving the previous equation for μ:

$$\mu = \frac{\pi(n_A\delta + \epsilon\delta)}{4M_0} \tag{21}$$

Substituting Eq. (19) in (21) result in,

$$\mu = \mu_0 \frac{n_A + \epsilon}{n_{A_0} + \epsilon_0} \tag{22}$$

The previous equation can be used to calculate the relay parameter μ required to obtain oscillations of a desired amplitude $\bar{A}_d = n_{A_d}\delta$ from the value of n_{A_0} obtained in previous oscillations using a relay with amplitude μ_0. Even though the actual value of ϵ_0 and ϵ are unknown, they are in interval $]0, 1[$. Therefore, in order to keep the amplitude of the oscillation as low as possible, it is assumed those values of ϵ_0 and ϵ for which the lowest value of μ is obtained, namely $\epsilon_0 = 1$ and $\epsilon = 0$, resulting in the following equation for calculating μ:

$$\mu = \mu_0 \frac{n_{A_d}}{n_{A_0} + 1} \tag{23}$$

Appendix C. Convergence of the procedure to identify the point C_1'

The goal of the procedure described on the steps 3 and 4 of the auto-tune algorithm proposed in Section 4 is to identify the point in the frequency response of $G(j\omega)I(j\omega)$ with phase $\phi_d = -3\pi/4$, that is $\phi_G(\omega_d) = -3\pi/4$, where $\phi_G(\omega)$ is the phase of $G(j\omega)I(j\omega)$. Because $\phi_G(\omega)$ is an unknown function, an iterative procedure is used to obtain points of $\phi_G(\omega)$ by introducing a time delay t_r whose value changes during the procedure. In each k iteration the value of $t_r(k)$ is calculated as follows:

$$t_r(k) = \frac{\phi_d + \pi}{\omega(k-1)} \tag{24}$$

The previous equation provides an approximate value of t_r to introduce the phase lag needed to induce oscillation in the point $\phi_G(\omega_d) = \phi_d$. This results from considering that the oscillation frequency obtained in the previous iteration, $\omega(n-1)$, is an approximate value of w_d. The time delay $t_r(k)$ is introduced to the system and a new relay feedback experiment is carried out, whose oscillatory response provides the value of $\omega(k)$ and $\phi_G(\omega(k)) = \omega(k)t_r(k)$ that are solution of the following equation:

$$\phi_G(\omega(k)) + \pi - t_r(k)\omega(k) = 0 \tag{25}$$

Once $w(k)$ is measured from the system response, it is used to calculate a new value of t_r to start the next iteration. The iterations continue until the desired point $\phi_G(\omega_d) = \phi_d$ is identified. Both Eqs. (24) and (25) are written according to Remark 4.

To analyze the convergence of this algorithm, the dynamic of the estimation error will be studied. To facilitate this study, the unknown function $\phi_G(\omega)$ is linearized around $\omega(k-1)$ according to the following expression:

$$\phi_G(\omega(k)) = \phi_G(\omega(k-1)) + \left.\frac{d\phi_G(\omega)}{d\omega}\right|_{\omega(k-1)} (\omega(k) - \omega(k-1)) \tag{26}$$

Eq. (24) is rewritten as follows:

$$\phi_d + \pi - t_r(k)\omega(k-1) = 0 \tag{27}$$

Substituting Eq. (26) in (25) and subtracting it from (27):

$$\phi_d - \phi_G(\omega(k-1)) = \left.\frac{d\phi_G(\omega)}{d\omega}\right|_{\omega(k-1)} (\omega(k) - \omega(k-1)) - t_r(k)(\omega(k) - \omega(k-1)) = 0 \tag{28}$$

Now, substituting Eq. (24) in (28) and defining $e_\phi(k-1) = \phi_d - \phi_G(\omega(k-1))$ and $\Delta_\omega(k) = \omega(k) - \omega(k-1)$:

$$e_\phi(k-1) = -\left[\frac{\phi_d + \pi}{\omega(k-1)} - \left.\frac{d\phi_G(\omega)}{d\omega}\right|_{\omega(k-1)}\right] \Delta_\omega(k) \tag{29}$$

The previous equation can be rewritten as:

$$\Delta_\omega(k) = -K_\phi e_\phi(k-1) \tag{30}$$

where

$$K_\phi = \frac{1}{\left[\frac{\phi_d+\pi}{\omega(k-1)} - \frac{d\phi_G(\omega)}{d\omega}\Big|_{\omega(k-1)}\right]} \tag{31}$$

Subtracting ϕ_d in both sides of Eq. (26) and substituting the expression of $\Delta_\omega(k)$ given by Eq. (30):

$$\phi_G(\omega(k)) - \phi_d = \phi_G(\omega(k-1)) - \phi_d + \frac{d\phi_G(\omega)}{d\omega}\Big|_{\omega(k-1)} (-K_\phi e_\phi(k-1)) \tag{32}$$

$$e_\phi(k) = e_\phi(k-1) - \frac{d\phi_G(\omega)}{d\omega}\Big|_{\omega(k-1)} (-K_\phi e_\phi(k-1)) \tag{33}$$

$$e_\phi(k) = e_\phi(k-1)\left[1 + \frac{d\phi_G(\omega)}{d\omega}\Big|_{\omega(k-1)} K_\phi\right] \tag{34}$$

From the previous equation, the condition for the asymptotic convergence of the algorithm to $e_\phi = 0$ is:

$$0 < \left[1 + \frac{d\phi_G(\omega)}{d\omega}\Big|_{\omega(k-1)} K_\phi\right] < 1 \tag{35}$$

That is,

$$-1 < \frac{d\phi_G(\omega)}{d\omega}\Big|_{\omega(k-1)} K_\phi < 0 \tag{36}$$

Substituting Eq. (31) in the inequality (36):

$$-1 < \frac{d\phi_G(\omega)}{d\omega}\Big|_{\omega(k-1)} \frac{1}{\left[\frac{\phi_d+\pi}{\omega(k-1)} - \frac{d\phi_G(\omega)}{d\omega}\Big|_{\omega(k-1)}\right]} < 0 \tag{37}$$

For most of the actual systems the phase response increase with the decrement of ω in the range starting from the phase crossover frequency, so $\frac{d\phi_G(\omega)}{d\omega}\Big|_{\omega(k-1)} < 0$. Furthermore, since $|\phi_d| < \pi$, then $\phi_d + \pi > 0$ and $\frac{\phi_d+\pi}{\omega(k-1)} > 0$. Therefore, the denominator of the central term in the expression (37) is positive and consequently can be operated without reversing the inequality. Taking this into account, the condition

$$\frac{d\phi_G(\omega)}{d\omega}\Big|_{\omega(k-1)} \frac{1}{\left[\frac{\phi_d+\pi}{\omega(k-1)} - \frac{d\phi_G(\omega)}{d\omega}\Big|_{\omega(k-1)}\right]} < 0 \tag{38}$$

can be reduced to

$$\frac{d\phi_G(\omega)}{d\omega}\Big|_{\omega(k-1)} < 0 \tag{39}$$

and condition

$$-1 < \frac{d\phi_G(\omega)}{d\omega}\Big|_{\omega(k-1)} \frac{1}{\left[\frac{\phi_d+\pi}{\omega(k-1)} - \frac{d\phi_G(\omega)}{d\omega}\Big|_{\omega(k-1)}\right]} \tag{40}$$

can be reduced to

$$\phi_d + \pi > 0 \tag{41}$$

As aforementioned, both conditions (39) and (41) are fulfilled. Hence, the procedure to identify the point C_1' convergence asymptotically to $e_\phi = 0$.

References

[1] Jan Lunze, Event-based control: Introduction and survey, in: M. Miskowicz (Ed.), Event-Based Control and Signal Processing, CRC Press, Boca Raton, 2015, pp. 3–20.

[2] Laura-Marie Feeney, Martin Nilsson, Investigating the energy consumption of a wireless network interface in an ad hoc networking environment, in: Proceedings IEEE INFOCOM 2001. Conference on Computer Communications. Twentieth Annual Joint Conference of the IEEE Computer and Communications Society (Cat. No. 01CH37213), Vol. 3, 2001, pp. 1548–1557.

[3] J. Sánchez, M. Guarnes, S. Dormido, A. Visioli, Comparative study of event-based control strategies: An experimental approach on a simple tank, in: 2009 European Control Conference, ECC, 2009, pp. 1973–1978.

[4] Marek Miskowicz, Send-on-delta concept: An event-based data reporting strategy, Sensors 6 (1) (2006) 49–63.

[5] Sebastián Dormido, José Sánchez, Ernesto Kofman, Muestreo, control y comunicación basados en eventos, Rev. Iberoam. Autom. Inform. Ind. RIAI 5 (1) (2008) 5–26.

[6] Joerns Ploennigs, Volodymyr Vasyutynskyy, Klaus Kabitzsch, Comparative study of energy-efficient sampling approaches for wireless control networks, IEEE Trans. Ind. Inform. 6 (3) (2010) 416–424.

[7] Manuel Beschi, Sebastián Dormido, José Sánchez, Antonio Visioli, Characterization of symmetric send-on-delta PI controllers, J. Process Control 22 (10) (2012) 1930–1945.

[8] Manuel Beschi, Sebastián Dormido, José Sánchez Moreno, Antonio Visioli, Luis José Yebra, Event-based PI plus feedforward control strategies for a distributed solar collector field, IEEE Trans. Control Syst. Technol. 22 (2014) 1615–1622.

[9] Andrzej Pawlowski, Manuel Beschi, José L. Guzmán, Antonio Visioli, Manuel Berenguel, Sebastián Dormido, Application of SSOD-PI and PI-SSOD event-based controllers to greenhouse climatic control, ISA Trans. 65 (2016) 525–536.
[10] Julio-Ariel Romero-Pérez, Roberto Sanchis-Llopis, Elena Arrebola, Experimental study of event based PID controllers with different sampling strategies. Application to brushless DC motor networked control system, in: 2015 XXV International Conference on Information, Communication and Automation Technologies, ICAT, 2015, pp. 1–6.
[11] Julio-Ariel Romero-Pérez, Roberto Sanchis-Llopis, A new method for tuning PI controllers with symmetric send-on-delta sampling strategy, ISA Trans. 64 (2016) 161–173.
[12] Oscar Miguel-Escrig, Julio-Ariel Romero-Pérez, Implementation and experimental evaluation of ssod sampling strategy for ebc, in: 2021 26th IEEE International Conference on Emerging Technologies and Factory Automation, ETFA, 2021, pp. 1–8.
[13] Oscar Miguel-Escrig Roberto Sanchis, Julio-Ariel Romero-Pérez, Experimental tuning of pi controllers with symmetric send-on-delta sampling from the step response, Internat. J. Control (2023) 1–10.
[14] Le Ye, Zhixuan Wang, Ying Liu, Peiyu Chen, Heyi Li, Hao Zhang, Meng Wu, Wei He, Linxiao Shen, Yihan Zhang, Zhichao Tan, Yangyuan Wang, Ru Huang, The challenges and emerging technologies for low-power artificial intelligence iot systems, IEEE Trans. Circuits Syst. I. Regul. Pap. 68 (12) (2021) 4821–4834, Cited by: 25.
[15] Yan Aiyun, Li Jingjiao, Jin Shuowei, Li Zhenni, A level crossing adc with variable symtem hysteresis, in: 2019 Chinese Control and Decision Conference, CCDC, 2019, pp. 1038–1042.
[16] Shuo-Wei Jin, Jing-Jiao Li, Zhen-Ni Li, A hysteresis comparator for level-crossing adc, in: 2017 29th Chinese Control and Decision Conference, CCDC, 2017, pp. 7753–7757.
[17] Manuel Beschi, Sebastián Dormido, José Sánchez, Antonio Visioli, Tuning of symmetric send-on-delta proportional-integral controllers, IET Control Theory Appl. 8 (11) (2014) 248–259.
[18] Oscar Miguel-Escrig, Julio-Ariel Romero-Pérez, Roberto Sanchis-Llopis, Tuning PID controllers with symmetric send-on-delta sampling strategy, J. Franklin Inst. 357 (2) (2020) 832–862.
[19] Oscar Miguel-Escrig, Julio-Ariel Romero-Pérez, Tuning procedure for event-based PI controllers under regular quantization with hysteresis, J. Franklin Inst. (2021).
[20] José Sánchez, María Guinaldo, Sebastián Dormido, Antonio Visioli, Validity of continuous tuning rules in event-based PI controllers using symmetric send-on-delta sampling: An experimental approach, Comput. Chem. Eng. (2020) 106878.
[21] Nikolai Mitrofanovich Krylov, Nikolai Nikolaevich Bogoliubov, Introduction to Non-Linear Mechanics, Princeton University Press, 1949.
[22] Yakov Z. Tsypkin, Relay Control Systems, Cambridge University Press, 1984.
[23] José Sánchez, María Guinaldo, Antonio Visioli, Sebastián Dormido, Enhanced event-based identification procedure for process control, Ind. Eng. Chem. Res. 57 (21) (2018) 7218–7231.
[24] José Sánchez, María Guinaldo, Antonio Visioli, Sebastián Dormido, Identification and tuning methods for PI control systems based on symmetric send-on-delta sampling, Int. J. Control Autom. Syst. 17 (11) (2019) 2784–2795.
[25] José Sánchez, María Guinaldo, Antonio Visioli, Sebastián Dormido, Identification of process transfer function parameters in event-based PI control loops, ISA Trans. 75 (2018) 157–171.
[26] John G. Ziegler, Nathaniel B. Nichols, Optimum settings for automatic controllers, Trans. ASME 64 (11) (1942).
[27] Karl J. Åström, Tore Hägglund, Revisiting the Ziegler–Nichols step response method for PID control, J. Process Control 14 (6) (2004) 635–650.
[28] Tore Hägglund, The one-third rule for PI controller tuning, Comput. Chem. Eng. 127 (2019) 25–30.
[29] Sigurd Skogestad, Simple analytic rules for model reduction and PID controller tuning, J. Process Control 13 (4) (2003) 291–309.
[30] Julio-Ariel Romero-Pérez, Roberto Sanchis-Llopis, Ignacio Peñarrocha-Alós, A simple rule for tuning event-based PID controllers with symmetric send-on-delta sampling strategy, in: Proceedings of the 2014 IEEE Emerging Technology and Factory Automation, ETFA, 2014, pp. 1–8.
[31] Oscar Miguel-Escrig, Julio-Ariel Romero-Pérez, Event-based discrete PI controllers robustness analysis through sampled describing function technique, Internat. J. Control (2021) 1–15.
[32] Julio-Ariel Romero-Pérez, Roberto Sanchis-Llopis, Analysis of a simple rule for tuning SSOD based PIDs, in: 2016 Second International Conference on Event-Based Control, Communication, and Signal Processing, EBCCSP, IEEE, 2016, pp. 1–8.
[33] Michael A. Johnson, Hohammad H. Moradi (Eds.), Chapter automatic PID controller tunning-the nonparametric approach, in: PID Control. New Identification and Design Methods, Springer, 2005, pp. 147–182.
[34] Julio Ariel Romero, Roberto Sanchis, Pedro Balaguer, Pi and pid auto-tuning procedure based on simplified single parameter optimization, J. Process Control 21 (6) (2011) 840–851.
[35] Li Sun, Donghai Li, Kwang Y. Lee, Optimal disturbance rejection for PI controller with constraints on relative delay margin, ISA Trans. 63 (2016) 103–111.